PNL-SA-25339

REAL-TIME DOSIMETRY FOR BORON-NEUTRON CAPTURE THERAPY

M. Bliss
R. A. Craig
P. L. Reeder
D. S. Sunberg

September 1994

Presented at the
First Workshop on Accelerator Based Boron Capture
Neutron Therapy
September 12-14, 1994
Jackson, Wyoming

Prepared for
the U.S. Department of Energy
under Contract DE-AC06-76RLO 1830

Pacific Northwest Laboratory
Richland, Washington 99352

DISCLAIMER

REAL-TIME DOSIMETRY FOR BORON-NEUTRON CAPTURE THERAPY

M. Bliss
R. A. Craig
P.L. Reeder
D. S. Sunberg

Pacific Northwest Laboratory, P.O. Box 999, Richland, WA 99352, USA, (509) 376-5578

Keywords: BNCT, dosimeter, scintillator

ABSTRACT

Epithermal/thermal boron neutron-capture therapy (BNCT) is a promising treatment method for malignant tumors. Because the doses and dose rates for medical therapeutic radiation are very close to the normal tissue tolerance, small errors in radiation delivery can result in harmful overdoses. A substantial need exists for a device that will monitor, in real time, the radiation dose being delivered to a patient.

Pacific Northwest Laboratory (PNL) has developed a scintillating glass optical fiber that is sensitive to thermal neutrons. The small size of the fibers offers the possibility of *in vivo* dose monitoring at several points within the radiation field. The count rate of such detectors can approach 10 MHz because the lifetime of the cerium activator is fast. Fluxes typical of those in BNCT (i.e., 10^9 n/cm^2/sec) may be measured because of this potentially high count rate and the small diameter of the fiber.

INTRODUCTION

Boron-neutron capture therapy (BNCT) offers the potential for significant reduction in dose to normal tissue because the neutron capture reaction results in the majority of the energy being deposited in the malignant cell. Dose rates in BNCT are, however, particularly difficult to calculate. Calculations must deal with beams that are a mix of neutrons of various energies. The cross-sections for the desired therapeutic reaction and reactions with natural nuclei in the patient are functions of the energy of the neutron and vary by several orders of magnitude for an epithermal beam mix. Thus, it would be highly desirable to have a real-time measure of dose rate at the delivery site that is also proportional to the other reaction rates of interest.

Current practice for BNCT dose measurement is to implant a gold wire at or near the tumor-treatment site. Part way through the treatment, the wire is removed and neutron-activated radionuclides are counted to determine the time required to complete the treatment.

This paper describes a concept for an alternative real-time dosimeter for BNCT. The basis for the dosimeter is a neutron-sensitive scintillating glass optical fiber. A conceptual design of a real-time dosimeter, a brief description of the physics of the sensor, nuclear and optical considerations, low-flux measurements collected using a single scintillating fiber, and design variations that are available to improve the performance of the basic detector design will be discussed.

CONCEPTUAL DESIGN

The design for the proposed real-time dosimeter is shown in Figure 1. The dosimeter consists of a short section of scintillating waveguide spliced to a chemically similar, passive waveguide. The passive waveguide carries the optical signal to a remote photon counter. The signal from the photon counter goes to a discriminator, passing only pulses which are greater in amplitude than some predetermined value. Because neutron events produce approximately an order of magnitude more photoelectrons than do gamma-ray interactions within the single scintillating waveguide, the threshold would be chosen such that counted pulses are unambiguously neutron events. These pulses then pass to a counting system which records pulse rate and total cumulative pulses. The active and passive waveguides would be suitably jacketed in a sterile, opaque, polyethylene sheath. The detector package, only a few hundred micrometers in diameter, would be inserted into the treatment site. Through calibration of a known neutron flux

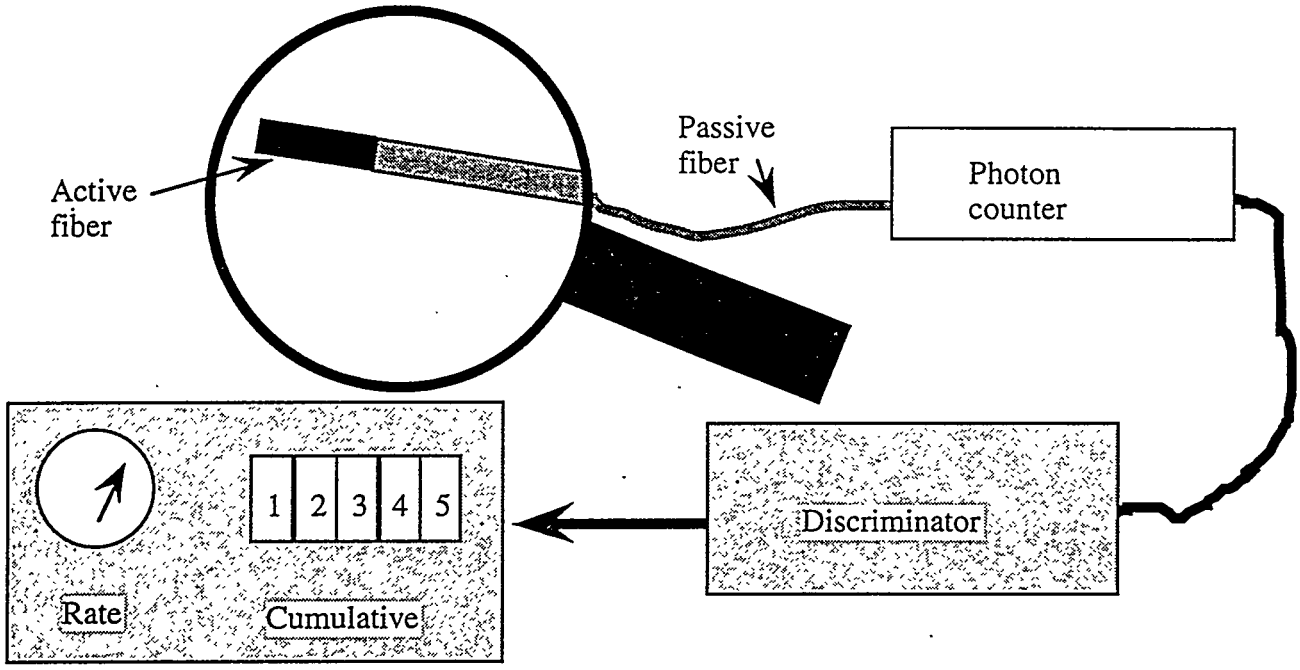

Figure 1. Conceptual design of real-time neutron dosimeter for use in BNCT relying on neutron-sensitive scintillating glass waveguides for the active element.

to pulses detected, unknown neutron fluxes can be determined. The optical elements of the detector are all extremely low-cost (the fiber elements cost a few dollars per meter) and would be single-use.

PHYSICS OF THE DETECTOR

The active portion of the sensor is based on detecting scintillation induced in the glass by a $^{6}Li(n,\alpha)^{3}H$ reaction. This reaction is exothermic, releasing approximately 4.7 MeV of which the majority is carried away by the triton (Figure 2). The triton and alpha both interact with the glass matrix to produce a trail of electronic excitations (ionization). These excitations can transfer energy by exciting Ce^{3+}, ions which will emit optical photons as they relax to the ground state.

The glass is a lithium aluminosilicate activated with cerium. The lithium is 97% enriched in ^{6}Li. It is well-known that this composition family scintillates in the presence of a thermal neutron flux.[1,2,3] This glass is drawn into a scintillating waveguide at Pacific Northwest Laboratory (PNL), using a hot downdraw fiberizing tower. The glass fiber is clad with a thermal-curing silicone that serves as both an optical cladding and a physical buffer. Fabricating this glass into fiber waveguides provides a new class of sensors for thermal neutron detection.[4,5,6,7,8] Successful fabrication of this sensor has been due in large part to superior oxidation-state control during the glassmaking and fiber-drawing activities.

An optical waveguide is formed when the fiber cladding has a smaller refractive index than that of the core. In this case, a fraction of the scintillation photons will be trapped in the fiber and guided towards each end. The fraction of the scintillation light that is captured is determined by the ratio of the cladding to core refractive index. For the silicone-clad, lithium-aluminosilicate fiber developed at PNL, this fraction is approximately 0.033 to each end.

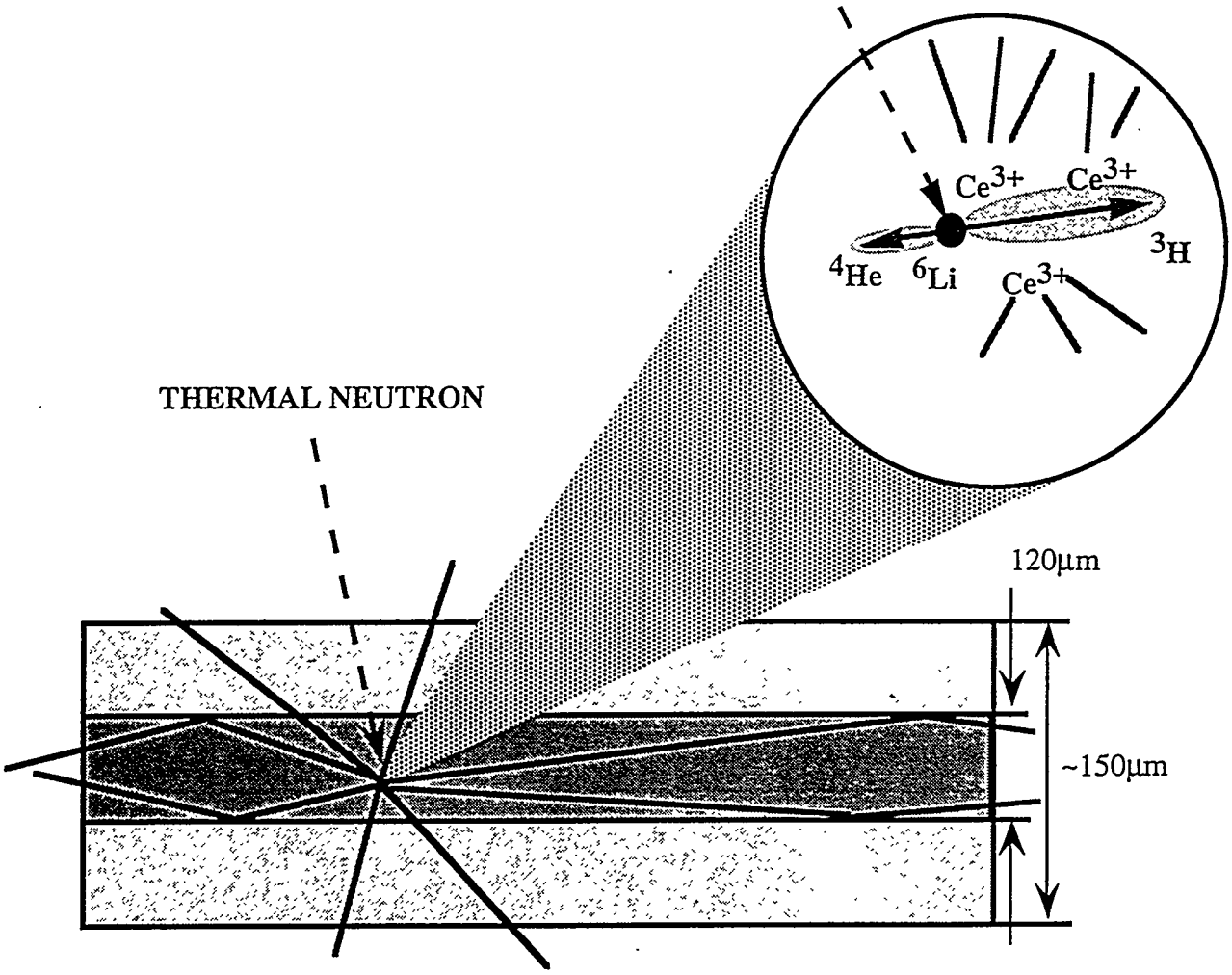

Figure 2. Schematic showing the major nuclear, electronic, and optical processes in the detection of a neutron with a scintillating-fiber waveguide.

NUCLEAR AND OPTICAL CONSIDERATIONS

Several questions must be addressed before seriously considering a single-fiber dosimeter:

1. Will the sensor saturate in the high-flux environment?
2. Will the sensor response be linear with respect to the dose to tissue?
3. Will the detector survive to provide the desired response over the time of treatment?
4. Will gamma-ray interactions result in interference?

Will the sensor saturate in the high-flux environment? To address this question, we consider the reaction rate for thermal neutrons incident onto a fiber. In an epithermal beam, the response rate for thermal neutrons will provide an upper bound to the actual rate. The quantity of material in a fiber 120 μm in diameter is approximately the same as that in a slab 120 μm wide and 94 μm thick. The neutron capture is affected by the amount of ^{6}Li in the glass. A typical glass composition is $0.25Li_2O \cdot 0.05Al_2O_3 \cdot 0.694SiO_2 \cdot 0.006Ce_2O_3$ in which the lithium is 97% enriched in ^{6}Li. A glass of this composition has a density of approximately 2.5 g/cm^3. Using this composition and the ^{6}Li thermal-neutron cross-section of 941 barns, a 120-μm-diameter fiber will capture approximately 11 percent of the thermal neutrons incident. For a single 120-μm-diameter fiber 1 cm long, the cross-sectional area seen by a neutron flux is 1.2×10^{-2} cm^2. Thus, the capture rate in a neutron flux of 10^9 neutrons/cm^2/sec by a fiber of this diameter and composition will be approximately 1.3×10^6 neutrons/sec per centimeter of fiber length; approximately 65% of the product tritons will deposit the full reaction energy in the fiber.

The scintillation decay curve for scintillation emission from Ce^{3+} activated glasses is multicomponent; the largest amplitude component has a decay time of 40 to 60 ns. Thus a pulse-shaping time of 0.1 to 1.0 μsec should suffice to provide a counting rate with excellent precision and linearity with respect to the reaction rate. The decay for Ce^{3+} does have significant long-time components; operationally, this results in single photons "dribbling out" for periods as long as microseconds after the initial event. Thus, pileup has to remain a concern in a high-flux environment. If the reaction rate at the desired neutron flux proves to be too high, it can be reduced by adjusting the active fiber length, the overall lithium content, or the lithium enrichment. If necessary, the count rate can be reduced by raising the pulse-height threshold to reduce the neutron efficiency.

Will the sensor response be linear with respect to the dose to tissue? The issue of whether the scintillating fiber response is proportional to dose centers around the neutron energy. The cross-section for the $^{6}Li(n,\alpha)^{3}H$ reaction is a function of neutron energy; so, too, are the cross-sections for the therapeutic $^{10}B(n,\alpha)^{7}Li$ reaction and the primary parasitic reactions: $^{14}N(n,p)$, and ^{23}Na neutron capture . Figure 3 shows the variation in cross-sections for these reactions as a function of incident neutron energy. From this, it is clear that the cross-sections for the therapeutic $^{10}B(n,\alpha)^{7}Li$ reaction and the $^{14}N(n,p)$ reaction vary with the square root of the energy in the same way as the $^{6}Li(n,\alpha)^{3}H$ reaction. Thus, the number of ^{6}Li neutron interactions is in proportion to the number of ^{10}B and ^{14}N reactions. Thus, the ^{6}Li fiber sensor provides all the necessary information to serve as an accurate and precise dosimeter. Additional information about the beam spectrum will be required to determine the rate of ^{23}Na neutron capture.

Will the detector survive to provide the desired response over the time of treatment? A remaining issue is that of radiation damage. Radiation damage occurs in glass because the excitations which represent ionization are capable of breaking bonds in the glass. Cerium is added

to glasses to protect them against radiation damage; the Ce^{3+}/Ce^{4+} redox reaction provides a means for dissipating the ionization without damage. Bulk samples of this glass, after exposure to extremely high doses (ca. 10^8 rad), at high dose rate, were noticeably darkened; in this state the scintillation efficiency was reduced significantly. However, the scintillation efficiency recovered completely after mild annealing. It is expected that the relatively small doses to the fiber (ca. 1000 rad) involved in a BNCT treatment session will not be sufficient to affect the dosimeter during a treatment. This remains to be demonstrated.

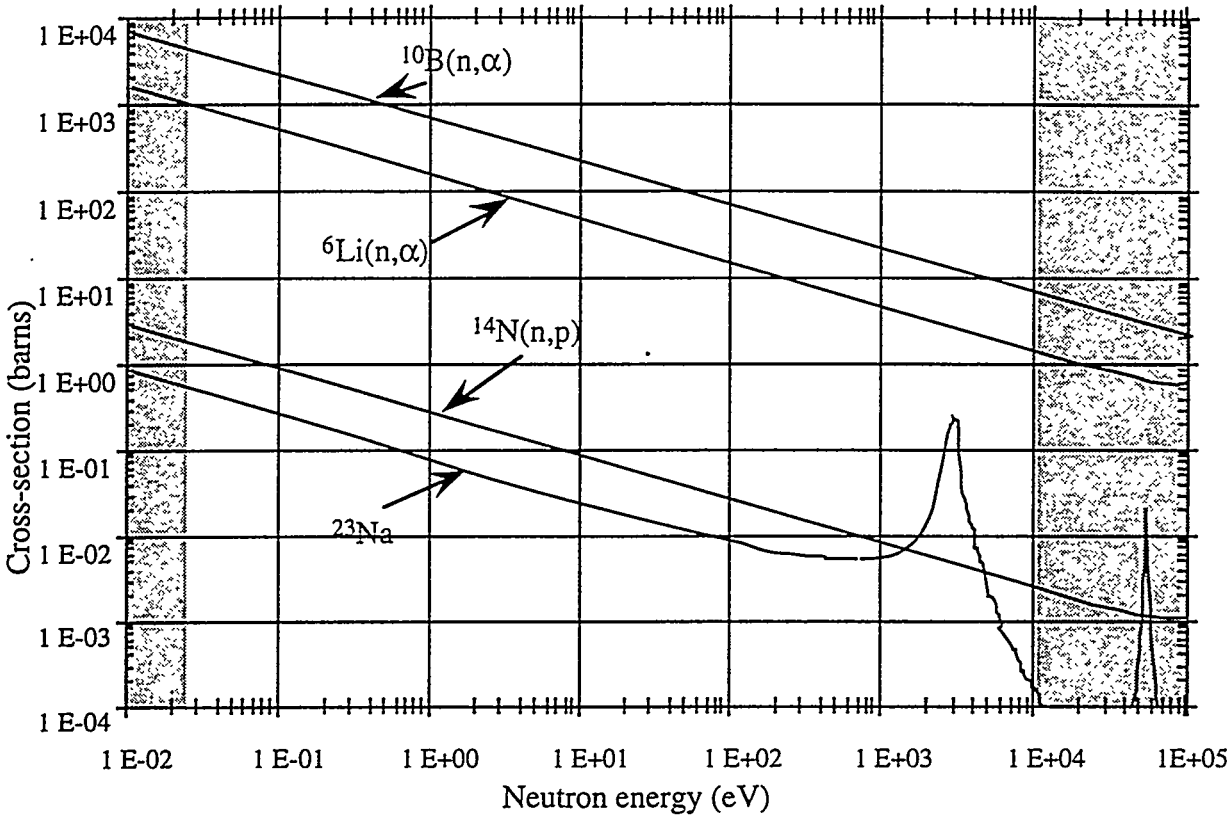

Figure 3. Variation of ^6Li, ^{10}B, and ^{14}N neutron-reaction cross-sections and ^{23}Na capture cross-section with neutron energy. The epithermal region is the unshaded area between the cold-neutron and high-energy-neutron regions.[9]

Will gamma-ray interactions result in interference? The detector will be operated in a mixed radiation field, including x-rays and gamma rays. Therefore, the question arises of interference from scintillation events caused by electromagnetic radiation. The key to successful discrimination between neutron and gamma-ray induced events is the ratio of initial photons produced.[a] The loss mechanisms are independent of the source of the photons and are the same for each.

The expected neutron and gamma-ray pulse-heights of the fiber system are governed by several factors: the scintillation efficiency, the numerical aperture of the fiber (that is, the index of refraction contrast between fiber and cladding), the transmission through the fiber and any inert

---

a Additionally, the gamma-ray flux is considerably smaller than that for the neutrons. Typical neutron fluxes are on the order of 10^9 n/cm^2-sec in a gamma-ray field of ca. 50 rad/hr. This corresponds to a flux of ca. 10^8 photons/cm^2-sec for 0.5 MeV photons.

fiber that may be in the light path, the loss at connections, and the photomultiplier efficiency as well as specifics of neutron and gamma interactions.

The scintillation efficiency of bulk glasses (of the compositions similar to that used in the glass fibers) has been measured to be as high as 9% of that for NaI crystals,[10,11] although more typical values are on the order of 6%. A typical neutron reaction produces scintillation equivalent to a 1.25-MeV electron.[12] Therefore, using the 6% glass relative efficiency and a NaI efficiency of 37,700 photons/MeV,[13] the bulk glass produces approximately 2800 photons. It has been found that, in fibers and unannealed samples, the scintillation efficiency is reduced. This is estimated to reduce the light output by approximately 35% in fibers. The refractive indices of the fiber and cladding are such that approximately 3% of all photons will be trapped within the fiber (each direction). Since the active fiber is short, fiber transmission loss can be neglected. Good mechanical splices should produce losses of less than one decibel; fiber-photomultipler coupling and photocathode efficiency are projected to be greater than 20%. This analysis is summarized in Table 1. The result is that a mean pulse height of nine photoelectrons for a neutron event is a reasonable expectation.

Table 1. Analysis of Expected Pulse Height Associated With a Scintillation Event in Fiber

	Photons Remaining	
	Neutron Event	Gamma Event
Initial Photon Production (Bulk; 6 % NaI)	2800	450
Fraction Produced in Fibers (= 0.65)	1840	290
Fraction Captured (= 0.033)	61	10
Fractional loss at 1-db splice (= 0.79)	48	8
PMT Coupling Factor (= 0.90)	43	7
PMT Quantum Efficiency (= 0.20)	9	1

In terms of interactions of the fiber with x-rays and gamma rays, several factors should be considered:

- X-rays and gamma rays interact with the fiber only through the particles that they produce (photoelectrons, Compton electrons, pair electrons and positrons).
- Because of their smaller linear energy transfer (LET), electrons and positrons have greater scintillation efficiency than heavier particles.
- The maximum amount of energy is deposited when a particle just stops in the fiber.
- In a single fiber, it is most unlikely for an electron with a range greater than the fiber diameter to deposit all its energy within the fiber. For energies up to approximately 0.5 MeV, the average energy deposited is less than 200 keV.

Taking 200 keV to be deposited by an electron the expected number of photoelectrons arising from an X-ray or gamma ray is analyzed in Table 1, using the same set of assumptions as used for the neutron event. The average photoelectron pulse height arising from such a mixed electromagnetic field is approximately one photoelectron. It should be noted that for the very unlikely event in which the full 0.5 MeV is deposited, the predicted pulse height is approximately three photoelectrons.

SINGLE-FIBER MEASUREMENTS

To test these analyses, the pulse heights were measured for a single fiber 97 cm (38 in.) long. Because the dark count rate in a single photomultiplier (PMT) is of the order of 400 counts per second, and the neutron count rate is projected to be 1 count per second for the small flux available, a coincidence arrangement was used (Figure 4). A 1-g PuBe source emitting ca. 8 x 10^4 neutrons/sec (into 4π) was used; to see the effect of exposure to beta particles, a ^{90}Sr source was substituted for the PuBe source and moderator. The sum of pulse heights in both PMTs provides the data shown in Figure 5. The peak at about Channel 8 corresponds to detection of one photoelectron in each PMT. The peak at Channel 40 in the neutron-induced pulse-height distribution corresponds to about five photoelectrons at each PMT. This is about a factor of 2 smaller than the estimate in Table 1 and can be explained by the measured transmission loss in the 97-cm-long fiber.

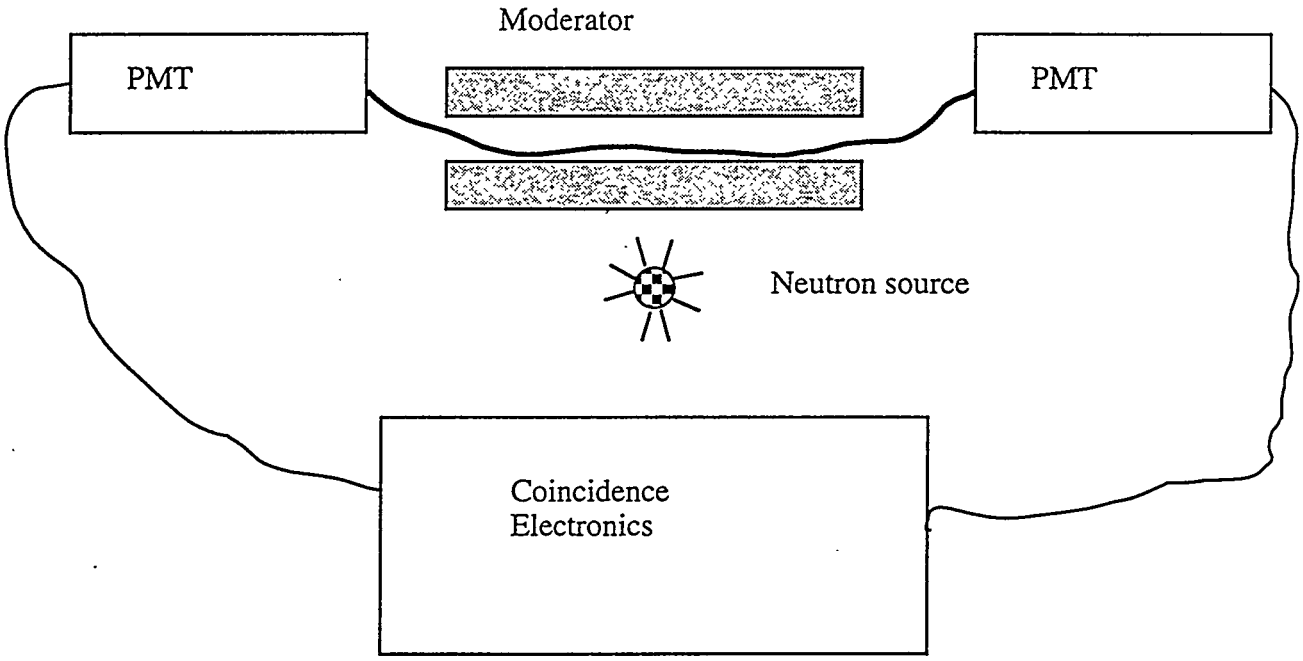

Figure 4. Experimental setup for measuring pulse-height distribution of neutron events in a single scintillating fiber.

DESIGN VARIATIONS

If desired or required, several variations on the simple conceptual dosimeter described above can improve on the overall performance of the dosimeter (Figure 6). The pulse height of the simple detector can be improved significantly by evaporating an aluminum mirror on the end. This

approach is routinely used on plastic fibers in the high-energy physics community and may increase the pulse height by as much as 90%. This will also increase the pulse height of x-ray and gamma-ray events and will increase the number of dribble-out photons.

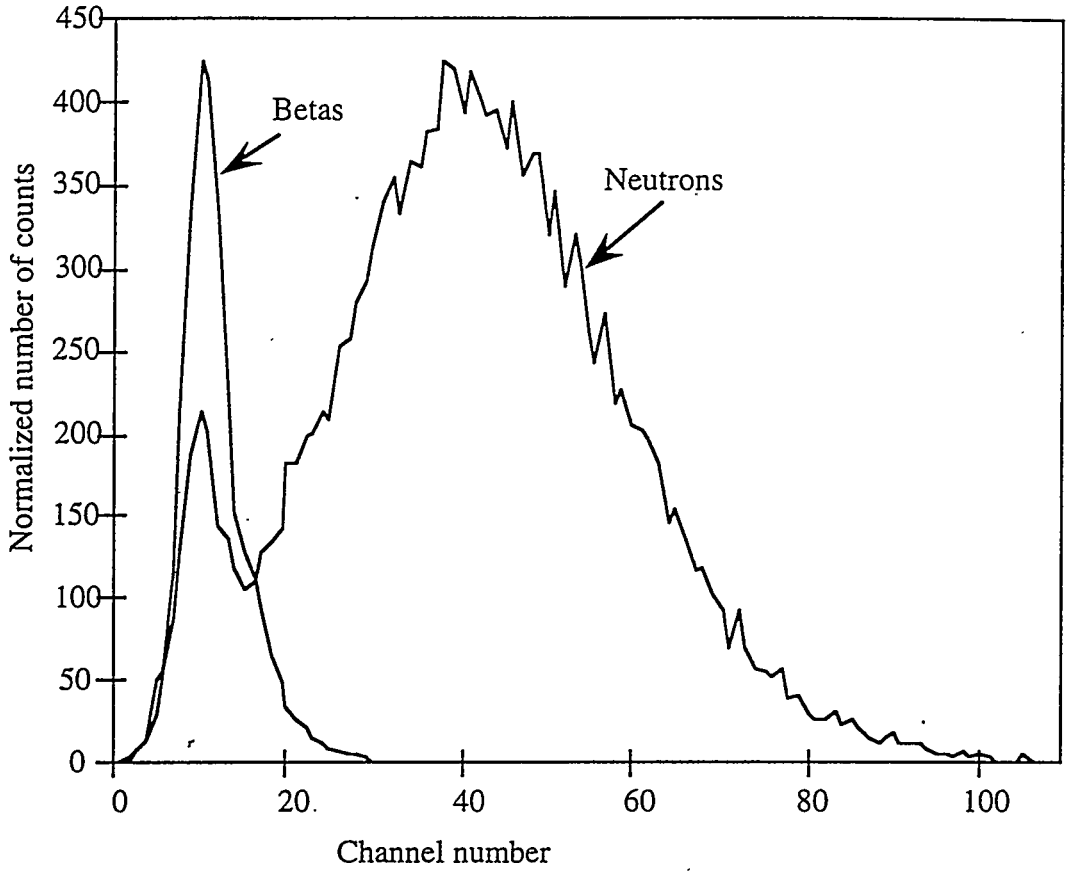

Figure 5. Pulse-height spectra of scintillating glass fibers in neutron and beta-ray fields.

If pulse-height discrimination does not suffice to unambiguously identify neutron events, a coincidence arrangement such as that shown in Figure 6 can be used. This requires a slightly more complicated fiber and electronics arrangement. In this case, the light from the distal end of the active fiber would be sent into a second passive fiber via a prism. Photons from both fibers would be sent to separate detectors operated in a coincidence mode. The further requirement that the pulse heights from both ends each exceed some predetermined value essentially eliminates x-ray and gamma-ray events and tube noise. This geometry would introduce additional losses at the coupling between the fibers and the prism; the tradeoff between 1) improved discrimination and 2) the increased loss and increased complexity will need careful assessment.

The conceptual design described in Section II is essentially a point detector. Position-dose information can easily be achieved by bundling fibers together. Seven 140-μm-diameter fibers can be bundled into a package 420 μm in diameter; 19 fibers can be bundled into a 700-μm-diameter package.

CONCLUSIONS AND ISSUES

The above analysis shows that a single cerium-activated lithium aluminosilicate fiber shows promise as a real-time dosimeter for boron-capture neutron therapy. It can provide a measure of the radiation dose, independent of the neutron energy in the epithermal regime, via ^{10}B and ^{14}N reactions (as well as any other reaction whose cross-section varies as $1/E^{1/2}$ in the epithermal region). The dosimeter is expected to be capable of operation in large neutron fluxes and in the presence of large x-ray and gamma-ray fluxes. Ultimately, of course, the question of whether the count rate is linear with the dose rate at high dose rates can only be answered by experimental calibrations. Options for improving dosimeter performance exist if the assumptions of the analysis prove to be excessively optimistic.

Possible remaining issues are whether single photoelectron events from late photons will cause a pile-up problem. If such is the case, ultrafast photon counting with appropriate electronic algorithms may be required to reject these counts. Much of this technology has already been developed for other applications. A remaining issue is that of radiation damage. Although radiation damage is very unlikely at such small doses, it has yet to be verified experimentally.

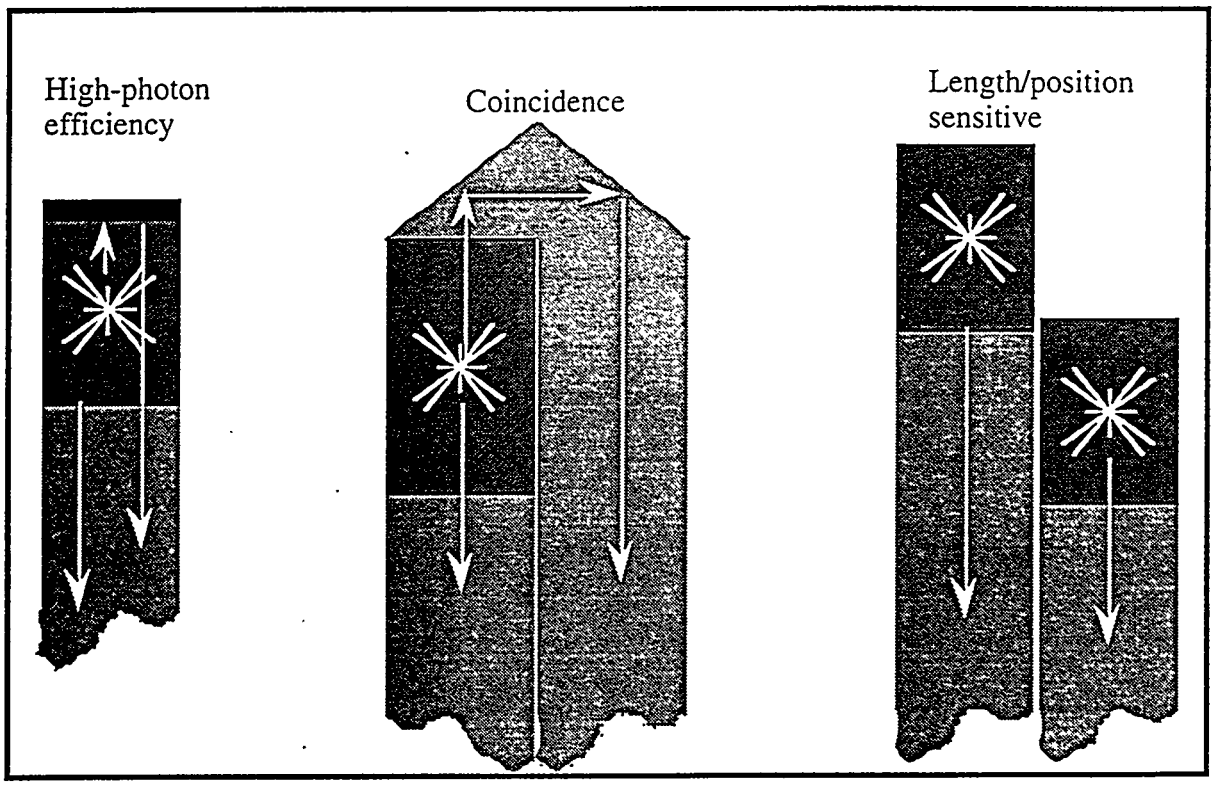

Figure 6. Possible variations on single-fiber dosimeter. The left figure shows a single fiber with a mirrored distal end to improve the pulse height. The center figure shows the light from the distal end of the active fiber being sent into a second passive fiber for coincidence measurements. The right figure shows how a cluster of fibers can be used to provide information about the neutron flux along the length of the detector.

ACKNOWLEDGEMENTS

This work was supported, in part, by Pacific Northwest Laboratory's Laboratory Directed Research and Development Program. The authors wish to thank W. C. Richey for his assistance with fiber fabrication and D. P. Brown for assistance with setting up the electronics. Pacific Northwest Laboratory is operated by Battelle Memorial Institute for the U. S. Department of Energy under Contract DE–AC06–76RLO 1830.

REFERENCES

1. R.J. Ginther, "New Cerium Activated Scintillating Glasses," IRE Trans. Nucl. Sci., **NS–7**, Nos. 2&3, 1960, 28.

2. L.M. Bollinger, G.E. Thomas, and R.J. Ginther, "Glass Scintillators for Neutron Detection," Nucl. Inst. Meth. **17** (1962) 97.

3. A.R. Spowart, "NEUTRON SCINTILLATING GLASSES: Part I," Nucl. Instr. and Meth. **135** (1976) 441.

4. G. Zanella and R. Zannoni, "X-ray Imaging with Scintillating Glass Optical Fibers," Nucl. Instr. Methods Phys. Res., **A287**, 619-627 (1990).

5. G.B. Spector, T. McCollum, and A.R. Spowart, "Scintillator fiber optic long counter for neutron detection," Nucl. Instr. Methods Phys. Res., **A309**, 303-317 (1991).

6. G.B. Spector, T. McCollum, and A.R. Spowart, "Advances in lithium-loaded glass scintillator fiber development," Nucl. Instr. Methods Phys. Res., **A313**, 373-376 (1992).

7. M. Atkinson, et al., "Initial Tests of a High Resolution Scintillating Fibre (SCIFI) Tracker," Nucl. Instr. Methods Phys. Res., **A254**, 500-514 (1987).

8. R. Ruchti, et al., "Scintillating Glass, Fiber-Optic Plate Detectors for Active Target and Tracking Applications in High Energy Physics Experiments," IEEE Transactions on Nuclear Science, **NS-31**, [1] 69-73 (1984).

9. Adapted from T. Nakagawa, et al. Eds., "Curves and Tables of Neutron Cross Sections", Japanese Atomic Energy Research Institute, JAERI-M 90-099, 1990.

10. M. Bliss, R.A. Craig D.S. Sunberg, and M.J. Weber, "Scintillators and Applications: Cerium-Doped Materials", Proceedings of EURODIM94 (Seventh Europhysical Conference on Defects in Materials), Lyon, France, July 5-8, 1994.

11. M. Bliss, R.A. Craig, P. L. Reeder, D.S. Sunberg, and M.J. Weber. "Relationship Between Microstructure and Efficiency of Scintillating Glasses", To be published in the Proceedings of the Materials Research Society Symposium on Scintillators, April 1994.

12. J.B. Birks, *The Theory and Practice of Scintillation Counting*, Pergamon, Oxford, 1964.

13. I. Holl, E. Lorenz, and G. Mageras, IEEE Trans. Nucl. Sci. 35, 105 (1988).